Research Article Vol. 36, No. 12 / December 2019 / Journal of the Optical Society of America A 2115

Journal of the Optical Society of America A

OPTICS, IMAGE SCIENCE, AND VISION

Estimating field-dependent nodal aberration theory coefficients from Zernike full-field displays by utilizing eighth-order astigmatism

ERIC M. SCHIESSER,* AARON BAUER, AND JANNICK P. ROLLAND

Institute of Optics, University of Rochester, 275 Hutchison Road, Rochester, New York 14627, USA
**Corresponding author: eric.schiesser@rochester.edu*

Received 22 August 2019; revised 23 October 2019; accepted 29 October 2019; posted 30 October 2019 (Doc. ID 376074); published 27 November 2019

When using freeform surfaces in optical design, the field dependence of the aberrations can become quite complex, and understanding these aberrations facilitates the design process. Here we calculate the field dependence of low-order Zernike astigmatism (Z5/6) up to the eighth order in nodal aberration theory (NAT). Expansion of NAT astigmatism terms to the eighth order facilitates a more accurate fit to the Zernike astigmatism data. We then show how this estimated field dependence can be used to quantitatively analyze a freeform telescope design. This analysis tool adds to the optical designer's arsenal when up against the challenge of designing with freeform optics.

https://doi.org/10.1364/JOSAA.36.002115

1. INTRODUCTION

The rising popularity of freeform optics has driven the creation of new design methods and aberration theories that can account for a lack of rotational symmetry. It is often convenient to represent the aberrations of a given optical system in terms of nodal aberration theory (NAT) [1,2]. To facilitate the use of freeform surfaces in the optical design of rotationally nonsymmetric optical systems, Fuerschbach *et al.* developed an extension to NAT, here called the aberration theory of freeform surfaces (ATFS) [3]. The ATFS predicts the aberrations of a given optical surface shape described by Zernike polynomial terms based on its location relative to a local pupil. Other works have proposed similar extensions of NAT by adding a pupil offset vector [4].

The ATFS, methods derived from it, and other nonrotationally symmetric aberration descriptions make use of full-field displays (FFDs), which show the magnitude and orientation of a given aberration over discrete points in the field of view (FOV) [5–7]. Bauer *et al.* show how to guide the design process using a visual, designer-guided semiquantitative assessment by examining Zernike FFDs to ascertain the aberration content of the optical system [5]. This method allows the designer to compare off-axis folding geometries and to decide which Zernike surface terms should be varied at a given step in the design based on the FFDs using ATFS and NAT.

Here we present a supporting method of freeform design based on both the principles in ATFS and the methods of Bauer *et al.* that uses a quantitative numerical analysis of the NAT aberration content from the underlying FFD data. This method is aided by an expansion of NAT to the eighth order for a more robust fit to the higher-order field-dependent aberrations that contribute to the Zernike astigmatism (Z5/6) FFDs.

In this work, we first expand the NAT wavefront expansion to the eighth order for terms that contribute higher-order field dependence to the Zernike astigmatism FFD. We then show that the field dependence of Zernike astigmatism can be determined by decomposing the FFD data into its constituent NAT aberration terms. Next, we show how this overall method can be used to determine the value of the surface coefficients required to correct certain NAT aberrations using ATFS. Finally, we show a design example of a three-mirror freeform telescope from the literature that illustrates both the FFD decomposition and the aberration correction through surface coefficient estimation.

2. EXPANSION OF NAT ASTIGMATISM TO THE EIGTH ORDER

NAT uses the vector formulation of Hopkins' wavefront expansion theorized by Shack and developed by Thompson with contributions from Buchroeder [8–11]. Individual NAT polynomial terms are determined by expanding the wavefront in terms of the field and pupil coordinate vectors and the sigma vector [12], which describes the aberration field centers. The general NAT wavefront in vector notation is given by Eq. (1), adapted from Thompson [[2], Eq. (42)], as follows:

$$W=\sum_{j}^{N}\sum_{p}^{\infty}\sum_{n}^{\infty}\sum_{m}^{\infty}[W_{k\ell m}]_j\left[\left(\vec{H}-\vec{\sigma}_j\right)\cdot\left(\vec{H}-\vec{\sigma}_j\right)\right]^p \times[\vec{\rho}\cdot\vec{\rho}]^n\left[\left(\vec{H}-\vec{\sigma}_j\right)\cdot\vec{\rho}\right]^m,$$

$$k=2p+m,\quad \ell=2n+m. \tag{1}$$

Thompson provides descriptions of spherical, coma, and astigmatism NAT aberrations up to the sixth order in the wavefront, where sixth order includes those terms for which $k+\ell\le 6$ [2,13–15]. Expanding this expression allows us to determine the field dependence of the various aberrations according to NAT. In design methods like that of Bauer *et al.*, a qualitative analysis of the aberration FFDs is used to understand the field dependence of the aberrations. To simplify the task of visually analyzing FFDs and to reduce the burden on the designer, we propose an analytical and quantitative way to determine the field dependence using the NAT aberration polynomial, which we describe in Section 3. However, because higher-order terms begin to dominate when the low-order aberration terms are corrected, sixth-order NAT terms may be insufficient to accurately describe the field dependence and, therefore, the expansion of Eq. (1) up to $k+\ell=8$ will be useful. When the lower-order aberration terms are corrected, the higher-order terms begin to dominate, and fitting with the sixth-order NAT polynomial can give a significant fit error (10% or more). Fitting with the eighth-order NAT polynomial reduces this fit error. Yet we are only interested in the terms that produce new types of higher-order field dependence. This is because fitting the FFD data to the NAT polynomial does not distinguish between terms with different $\vec{\sigma}$ or ρ^2 dependence, only field dependence ($\vec{H}$). Since the astigmatism FFD data is showing the Zernike aberrations over the field of view, terms with different $\vec{\sigma}$ or ρ^2 dependence but the same field dependence ($\vec{H}$) cannot be distinguished in the FFD, since the FFD only shows the field dependence. The Zernike Z5/6 (astigmatism) FFD shows the sum of the $\vec{\rho}^2$-dependent terms [see Eq. (41)]. Therefore, the eighth-order terms that exhibit the same field dependence as the lower-order terms are dropped from the expansion, since they do not contribute new field dependence that is not already accounted for by the fourth-or sixth-order expansion as we describe in Section 3.

Note that in this work we refer to the "order" of aberrations by the wavefront order, in contrast to the optical terminology that considers wavefront expansions to the fourth order as "thirrd-order" and sixth-order expansions as "fifth-order," etc. The latter terminology refers to the combined aperture and field dependence of the ray aberration coefficients, which we do not consider in this work, so we have persisted with the wavefront order.

A. Field Dependence of Zernike Astigmatism (Z_5 and Z_6) Up to the Eighth Order

To determine the eighth-order NAT field dependence of the Zernike aberrations, we first expand the NAT wavefront to the eighth order. In this work, we focus on low-order Zernike astigmatism (Z5 and Z6 in FRINGE ordering) since it is often the largest aberration of off-axis or tilted component systems. Additionally, according to ATFS, all low-order Zernike freeform surface shapes contribute to the field dependence of Zernike astigmatism in general, except in the special case of the shape being located at the stop surface, so it is critical to have a quantitative understanding of it for freeform design.

To analytically understand the astigmatism terms with higher-order field dependence, we can examine the difference between the NAT astigmatism terms for expansion through the sixth order and through the eighth order. The sixth-order terms are those terms where $k+\ell=6$, and the eighth-order terms have $k+\ell=8$, which we have denoted in the subscripts as follows:

$$W_{k+l=6,m=2}=\sum_{j=1}^{n}W_{242,j}\left[\left(\vec{H}-\vec{\sigma}_j\right)\cdot\left(\vec{H}-\vec{\sigma}_j\right)\right]^0\times[\vec{\rho}\cdot\vec{\rho}]^1\left[\left(\vec{H}-\vec{\sigma}_j\right)\cdot\vec{\rho}\right]^2+\sum_{j=1}^{n}W_{422,j}\left[\left(\vec{H}-\vec{\sigma}_j\right)\cdot\left(\vec{H}-\vec{\sigma}_j\right)\right]^1\times[\vec{\rho}\cdot\vec{\rho}]^0\left[\left(\vec{H}-\vec{\sigma}_j\right)\cdot\vec{\rho}\right]^2, \tag{2}$$

$$W_{k+l=8,m=2}=\sum_{j=1}^{n}W_{262,j}\left[\left(\vec{H}-\vec{\sigma}_j\right)\cdot\left(\vec{H}-\vec{\sigma}_j\right)\right]^0\times[\vec{\rho}\cdot\vec{\rho}]^2\left[\left(\vec{H}-\vec{\sigma}_j\right)\cdot\vec{\rho}\right]^2+\sum_{j=1}^{n}W_{442,j}\left[\left(\vec{H}-\vec{\sigma}_j\right)\cdot\left(\vec{H}-\vec{\sigma}_j\right)\right]^1\times[\vec{\rho}\cdot\vec{\rho}]^1\left[\left(\vec{H}-\vec{\sigma}_j\right)\cdot\vec{\rho}\right]^2+\sum_{j=1}^{n}W_{622,j}\left[\left(\vec{H}-\vec{\sigma}_j\right)\cdot\left(\vec{H}-\vec{\sigma}_j\right)\right]^2\times[\vec{\rho}\cdot\vec{\rho}]^0\left[\left(\vec{H}-\vec{\sigma}_j\right)\cdot\vec{\rho}\right]^2. \tag{3}$$

It is worth noting here that Thompson treats W_{242} as an oblique spherical aberration [13]. We include it here because, as Thompson also notes: "It is in fact exactly third-order astigmatism with an aperture to the fourth dependence, characteristic of third-order spherical aberration." Therefore, W_{242} terms will contribute to the Z5/6 field dependence. Additionally, Thompson considers field curvature terms and astigmatism terms in the same treatment [15]. Because here we consider only terms contributing to Z5/6 field dependence, we do not consider the field curvature terms in the expansion.

The sixth-order astigmatism expansion terms are generated from Eq. (2), and the eighth-order astigmatism terms are generated from Eq. (3). Comparing the first lines and the second lines of each equation, we see that they produce the same field dependence in the sixth order and eighth order since they differ

only by a ρ^2 factor. Furthermore, we can see that higher-order field dependence will be produced by the third line of Eq. (3). We can expand this line to determine the new field-dependent terms as follows:

$$\begin{aligned}&\sum_{j=1}^{n} W_{622,j}\left[\left(\vec{H}-\vec{\sigma}_j\right)\cdot\left(\vec{H}-\vec{\sigma}_j\right)\right]^2[\vec{\rho}\cdot\vec{\rho}]^0\left[\left(\vec{H}-\vec{\sigma}_j\right)\cdot\vec{\rho}\right]^2\\&=\sum_{j=1}^{n} W_{622,j}\left[H^2+\sigma_j^2-2\left(\vec{H}\cdot\vec{\sigma}_j\right)\right]^2\left[\vec{H}\cdot\vec{\rho}-\vec{\sigma}_j\cdot\vec{\rho}\right]^2\\&=\sum_{j=1}^{n} W_{622,j}\Big[H^4+\sigma_j^4+4\left(\vec{H}\cdot\vec{\sigma}_j\right)^2+2H^2\sigma_j^2\\&\quad-4H^2\left(\vec{H}\cdot\vec{\sigma}_j\right)-4\sigma_j^2\left(\vec{H}\cdot\vec{\sigma}_j\right)\Big]\ldots\\&\quad\times\left[\left(\vec{H}\cdot\vec{\rho}\right)^2+\left(\vec{\sigma}_j\cdot\vec{\rho}\right)^2-2\left(\vec{H}\cdot\vec{\rho}\right)\left(\vec{\sigma}_j\cdot\vec{\rho}\right)\right].\end{aligned}\tag{4}$$

At this stage, it is helpful to introduce a vector identity involving the Shack vector product (SVP) that allows us to group terms according to field dependence [11,16] as follows:

$$2\left(\vec{A}\cdot\vec{B}\right)\left(\vec{A}\cdot\vec{C}\right)=\left(\vec{A}\cdot\vec{A}\right)\left(\vec{B}\cdot\vec{C}\right)+\vec{A}^2\cdot\vec{B}\vec{C}.\tag{5}$$

Applying this identity to the last term in Eq. (4) yields two terms as follows:

$$2\left(\vec{H}\cdot\vec{\rho}\right)\left(\vec{\sigma}_j\cdot\vec{\rho}\right)=\left(\vec{H}\cdot\vec{\sigma}_j\right)\rho^2+\left(\vec{H}\vec{\sigma}_j\right)\cdot\vec{\rho}^2.\tag{6}$$

A special case of Eq. (5) where $\vec{B}=\vec{C}$ is also useful is

$$\begin{aligned}2\left(\vec{A}\cdot\vec{B}\right)^2&=\left(\vec{A}\cdot\vec{A}\right)\left(\vec{B}\cdot\vec{B}\right)+\vec{A}^2\cdot\vec{B}^2\\&=A^2B^2+\vec{A}^2\cdot\vec{B}^2.\end{aligned}\tag{7}$$

Applying Eq. (7) to the relevant terms in Eq. (4) yields two terms each, one field curvature and one astigmatism term as follows:

$$\left(\vec{H}\cdot\vec{\rho}\right)^2=\frac{1}{2}H^2\rho^2+\frac{1}{2}\vec{H}^2\cdot\vec{\rho}^2,\tag{8}$$

$$\left(\vec{\sigma}_j\cdot\vec{\rho}\right)^2=\frac{1}{2}\sigma_j^2\rho^2+\frac{1}{2}\vec{\sigma}_j^2\cdot\vec{\rho}^2,\tag{9}$$

$$\left(\vec{H}\cdot\vec{\sigma}_j\right)^2=\frac{1}{2}H^2\sigma_j^2+\frac{1}{2}\vec{H}^2\cdot\vec{\sigma}_j^2.\tag{10}$$

To further simplify the algebra, we can examine the Zernike Z5/6 polynomial and compare it with the ρ dependence in Eq. (4) in the light of Eqs. (8)–(6) as follows:

$$Z_5\propto\rho^2\cos 2\phi=\vec{\rho}^2\cdot\hat{x},\tag{11}$$

$$Z_6\propto\rho^2\sin 2\phi=\vec{\rho}^2\cdot\hat{y}.\tag{12}$$

Any terms in Eq. (4) that do not have $\vec{\rho}^2$ dependence will not contribute to the $Z_{5/6}$ FFD, and therefore we can ignore them for the purposes of this exercise. Thus, we drop the first term on the right-hand side of Eqs. (6), (8), and (9). Applying the identities to Eq. (4) and dropping the irrelevant terms therefore yields

$$\begin{aligned}[W]_{622}^{Z_{5/6}}&=\sum_{j=1}^{n} W_{622,j}\Big[H^4+\sigma_j^4+4H^2\sigma_j^2+2\vec{H}^2\cdot\vec{\sigma}_j^2\\&\quad-4H^2\left(\vec{H}\cdot\vec{\sigma}_j\right)-4\sigma_j^2\left(\vec{H}\cdot\vec{\sigma}_j\right)\Big]\ldots\\&\quad\times\left[\frac{1}{2}\vec{H}^2\cdot\vec{\rho}^2+\frac{1}{2}\vec{\sigma}_j^2\cdot\vec{\rho}^2-\left(\vec{H}\vec{\sigma}_j\right)\cdot\vec{\rho}^2\right].\end{aligned}\tag{13}$$

We denote the wavefront expansion $[W]_{622}^{Z_{5/6}}$ with the superscript $Z_{5/6}$ to refer to those NAT wavefront terms that contribute to the Zernike astigmatism aberrations, Z5 and Z6. The bracketed term $[W]_{622}$ is used to denote a shorthand for the NAT wavefront expansion for the terms related to the Hopkins W_{622} term, similar to the shorthand used in [2]. To dissect and better understand Eq. (13), it is instructive to gather the terms according to their "order" of field dependence.

1. Sixth-Order Field Dependence

Only one term will contribute sixth-order dependence according to Eq. (13) as follows:

$$W_{622,6^{\text{th}}\text{Order}}^{Z_{5/6}}=\frac{1}{2}\sum_{j=1}^{n} W_{622,j}H^4\vec{H}^2\cdot\vec{\rho}^2.\tag{14}$$

Note that this term has no $\vec{\sigma}_j$ dependence. This is simply the "normal" rotationally symmetric eighth-order astigmatism term expressed in the appropriate NAT vector format.

2. Fifth-Order Field Dependence

There are two terms that contribute to the fifth-order field dependence:

$$\begin{aligned}&W_{622,5^{\text{th}}\text{Order}}^{Z_{5/6}}\\&=-\sum_{j=1}^{n} W_{622,j}H^2\left[H^2\left(\vec{H}\vec{\sigma}_j\right)+2\left(\vec{H}\cdot\vec{\sigma}_j\right)\vec{H}^2\right]\cdot\vec{\rho}^2.\end{aligned}\tag{15}$$

We then define the eighth-order NAT coefficient $\vec{A}_{622}$:

$$\vec{A}_{622}\equiv\sum_{j=1}^{n} W_{622,j}\vec{\sigma}_j.\tag{16}$$

This gives the final fifth-order representation:

$$\begin{aligned}&W_{622,5^{\text{th}}\text{Order}}^{Z_{5/6}}\\&=-\sum_{j=1}^{n} H^2\left[H^2\left(\vec{H}\vec{A}_{622,j}\right)+2\left(\vec{H}\cdot\vec{A}_{622,j}\right)\vec{H}^2\right]\cdot\vec{\rho}^2.\end{aligned}\tag{17}$$

3. Fourth-Order Field Dependence

At first glance, there appear to be four fourth-order terms:

$$W^{Z_{5/6}}_{622,4^{\text{th}}\text{Order}} = \sum_{j=1}^{n} W_{622,j}\left[\frac{1}{2}H^4\vec{\sigma}_j^2 + 2H^2\sigma_j^2\vec{H}^2 + \left(\vec{H}^2\cdot\vec{\sigma}_j^2\right) \times \vec{H}^2 + 4H^2\left(\vec{H}\cdot\vec{\sigma}_j\right)\left(\vec{H}\vec{\sigma}_j\right)\right]\cdot\vec{\rho}^2. \tag{18}$$

We define three sigma dependences:

$$B_{622} \equiv \sum_{j=1}^{n} W_{622,j}\sigma_j^2, \tag{19}$$

$$\vec{B}^2_{622} \equiv \sum_{j=1}^{n} W_{622,j}\vec{\sigma}_j^2, \tag{20}$$

$$\vec{B}^{2*}_{622} \equiv \sum_{j=1}^{n} W_{622,j}\left(\vec{\sigma}_j^*\right)^2. \tag{21}$$

Combining these definitions and the identities in Eqs. (A4) and (A5) provided in Appendix A with Eq. (18) yields the fourth-order terms:

$$W^{Z_{5/6}}_{622,4^{\text{th}}\text{Order}} = \sum_{j=1}^{n}\left[3H^4\vec{B}^2_{622,j} + 4B_{622,j}H^2\vec{H}^2 + \frac{1}{2}\vec{H}^4\vec{B}^{2*}_{622,j}\right]\cdot\vec{\rho}^2. \tag{22}$$

4. Third-Order Field Dependence

There appear to be four third-order terms:

$$W^{Z_{5/6}}_{622,3^{\text{rd}}\text{Order}} = \sum_{j=1}^{n} W_{622,j}\begin{bmatrix} -4H^2\sigma_j^2\left(\vec{H}\vec{\sigma}_j\right) - 2\vec{H}^2\cdot\vec{\sigma}_j^2\left(\vec{H}\vec{\sigma}_j\right)\ldots \\ -2H^2\left(\vec{H}\cdot\vec{\sigma}_j\right)\vec{\sigma}_j^2 - 2\sigma_j^2\left(\vec{H}\cdot\vec{\sigma}_j\right)\vec{H}^2\end{bmatrix}\cdot\vec{\rho}^2. \tag{23}$$

However, we can apply the identities in Eqs. (A6)–(A9) to simplify to only three terms. We define the following sigma-dependent aberration coefficients:

$$\vec{C}^3_{622} \equiv \sum_{j=1}^{n} W_{622,j}\vec{\sigma}_j^3, \tag{24}$$

$$\vec{C}_{622} \equiv \sum_{j=1}^{n} W_{622,j}\sigma_j^2\vec{\sigma}_j, \tag{25}$$

$$\vec{C}^*_{622} \equiv \sum_{j=1}^{n} W_{622,j}\sigma_j^2\vec{\sigma}_j^*. \tag{26}$$

Collecting all the terms, considering the identities and definitions, we get the third-order field-dependent terms:

$$W^{Z_{5/6}}_{622,3^{\text{rd}}\text{Order}} = -\sum_{j=1}^{n}\left[6H^2\vec{H}\vec{C}_{622,j} + 2H^2\vec{H}^*\vec{C}^3_{622,j} + 2\vec{H}^3\vec{C}^*_{622,j}\right]\cdot\vec{\rho}^2. \tag{27}$$

5. Second-Order Field Dependence

The second order has four terms that can be simplified to three terms while separating the field dependence from the sigma dependence:

$$W^{Z_{5/6}}_{622,2^{\text{nd}}\text{Order}} = \sum_{j=1}^{n} W_{622,j}\left[\frac{1}{2}\sigma_j^4\vec{H}^2 + 2H^2\sigma_j^2\vec{\sigma}_j^2 + \left(\vec{H}^2\cdot\vec{\sigma}_j^2\right)\vec{\sigma}_j^2 + 4\sigma_j^2\left(\vec{H}\cdot\vec{\sigma}_j\right)\vec{H}\vec{\sigma}_j\right]\cdot\vec{\rho}^2. \tag{28}$$

The first two terms are already separated. The third and fourth terms can be separated and combined with the others using Eqs. (A10) and (A11). There are three sigma-dependent terms to define:

$$D_{622} = \sum_{j=1}^{n} W_{622,j}\sigma_j^4, \tag{29}$$

$$\vec{D}^2_{622} = \sum_{j=1}^{n} W_{622,j}\sigma_j^2\vec{\sigma}_j^2, \tag{30}$$

$$\vec{D}^4_{622} = \sum_{j=1}^{n} W_{622,j}\vec{\sigma}_j^4. \tag{31}$$

Combining the terms and substituting the definitions, we get the second-order field-dependent terms:

$$W^{Z_{5/6}}_{622,2^{\text{nd}}\text{Order}} = \sum_{j=1}^{n}\left[3D_{622,j}\vec{H}^2 + 4H^2\vec{D}^2_{622,j} + \frac{1}{2}\vec{H}^{2*}\vec{D}^4_{622,j}\right]\cdot\vec{\rho}^2. \tag{32}$$

6. First-Order Field Dependence

We have

$$W^{Z_{5/6}}_{622,1^{\text{st}}\text{Order}} = -\sum_{j=1}^{n} W_{622,j}\left[\sigma_j^4\left(\vec{H}\vec{\sigma}_j\cdot\vec{\rho}^2\right) + 2\sigma_j^2\left(\vec{H}\cdot\vec{\sigma}_j\right)\left(\vec{\sigma}_j^2\cdot\vec{\rho}^2\right)\right]. \tag{33}$$

The second term can be separated into two terms based on field and sigma dependence and combined with the first term using Eq. (A12). We now have two fifth-order sigma-dependent terms to define:

$$\vec{E}_{622} \equiv \sum_{j=1}^{n} W_{622,j}\sigma_j^4\vec{\sigma}_j, \tag{34}$$

$$\vec{E}^3_{622} \equiv \sum_{j=1}^{n} W_{622,j}\sigma_j^2\vec{\sigma}_j^3. \tag{35}$$

Combining the terms and applying the definitions, we get the first-order field-dependent terms:

$$W^{Z_{5/6}}_{622,1^{st}\text{Order}} = -\sum_{j=1}^{n}\left[2\vec{E}_{622,j}\vec{H} + \vec{E}^3_{622,j}\vec{H}^*\right]\cdot\vec{\rho}^2. \tag{36}$$

7. Field-Constant Dependence

We have

$$W^{Z_{5/6}}_{622,\text{Const}} = \frac{1}{2}\sum_{j=1}^{n} W_{622,j}\sigma_j^4\left(\vec{\sigma}_j^2\cdot\vec{\rho}^2\right). \tag{37}$$

There is no field dependence to separate in this case, but we do need to define a new sigma-dependent term:

$$\vec{F}^2_{622} = \sum_{j=1}^{n} W_{622,j}\sigma_j^4\vec{\sigma}_j^2. \tag{38}$$

Thus, the field-constant eighth-order term is given by

$$W^{Z_{5/6}}_{622,\text{Const}} = \sum_{j=1}^{n}\frac{1}{2}\vec{F}^2_{622,j}\cdot\vec{\rho}^2. \tag{39}$$

8. New Field Dependence of Eighth-Order NAT Astigmatism

Some of the terms from Eqs. (14), (17), (22), (27), (32), (36), and (39) have higher-order field dependence compared to the sixth-order expansion terms, but some are simply new combinations of sigma and field dependence. The relevant polynomial for the purposes of this work is constructed by collecting all the fourth-and sixth-order expansion terms and adding in the new field dependence from the eighth-order expansion as follows:

$$W^{k+\ell\le 8}_{Z_{5/6}} = \frac{1}{2}\left\{\begin{array}{l}\left[W_{222} + W_{422}H^2 + \boldsymbol{W_{622}H^4} - 2\vec{H}\cdot\left(\left(\vec{A}_{422}\right) + \boldsymbol{2H^2\vec{A}_{622}}\right)\right]\vec{H}^2\ldots \\ +3H^2\vec{B}_{422} + \boldsymbol{6H^4\vec{B}^2_{622}} + \boldsymbol{\vec{H}^4\vec{B}^{2*}_{622}}\ldots \\ -2\left(\vec{A}_{222} + H^2\left(\vec{A}_{422} + \boldsymbol{3\vec{C}_{622}}\right) + \boldsymbol{H^4\vec{A}_{622}}\right)\vec{H}\ldots \\ -\vec{C}^3_{422}\vec{H}^* \boldsymbol{-4\,H^2\vec{H}^*\vec{C}^3_{622}} \boldsymbol{-4\,\vec{H}^3\vec{C}^*_{622}} + \boldsymbol{\vec{D}^4_{622}\vec{H}^{2*}} + \vec{B}^2_{222}\end{array}\right\}\cdot\vec{\rho}^2. \tag{40}$$

Note that only the lowest-order field-dependent term is included in Eq. (40), e.g., only the field-constant fourth-order expansion term is included, and the field-constant sixth-order term is excluded. The new field-dependent terms from the eighth-order expansion are in **bold** text in Eq. (40).

3. FITTING THE $Z_{5/6}$ FFD WITH NAT FIELD DEPENDENCE

Recent design methods relying on ATFS use the Zernike FFD as a guide for the designer to determine the limiting aberration in a given design [3,5]. The limiting aberration is then corrected using a certain surface shape according to ATFS. These methods rely on a qualitative analysis of the FFD and the designer's knowledge of ATFS. Many high-performance reflective freeform systems have been designed and even fabricated using this method [17–20]. However, the designer may find it advantageous to be able to determine exactly how much of a given NAT aberration is present in a system. Furthermore, armed with this information, a designer could predict the magnitude of a given Zernike surface shape to add to a given surface. In this section, we will show this is possible using the field dependence of the Zernike astigmatism FFD shown in Eq. (40).

To estimate the NAT aberrations in an optical system, we can fit the Zernike FFD data with the NAT polynomial. This method is similar to that of Gray *et al.*, where Gray performed a similar analysis for the standard rotationally symmetric wavefront expansion [21]. Said another way, we can expand the NAT wavefront polynomial in terms of the Zernike polynomials. The coefficients of each Zernike polynomial term will be determined by the following integral (adapted from [21]):

$$z_n\left(\vec{H};\vec{\sigma}_j\right) = \frac{1}{N_n}\int_0^{2\pi}\int_0^1 W\left(\vec{H},\vec{\rho};\vec{\sigma}_j\right)Z_n\left(\vec{\rho}\right)\rho\mathrm{d}\rho\mathrm{d}\phi. \tag{41}$$

Here we have used the FRINGE ordering of the Zernike polynomials [22]. We are interested in the coefficients of the astigmatism terms ($Z_{5/6}$) of the Zernike polynomial given by Eqs. (11) and (12). In the light of these equations, the only terms in the NAT wavefront polynomial that will be non-zero following the integral of Eq. (41) for Z_5 and Z_6 will be terms that depend on the $\hat{x}$ or $\hat{y}$ components of $\vec{\rho}^2$, respectively. Because of the dot product with $\vec{\rho}^2$ in Eq. (40), all of the $\hat{x}$ components of the left side of that dot product will be non-zero in the Z_5 integral, and the $\hat{y}$ components will be non-zero in the Z_6 integral. Therefore, for the purposes of our fitting algorithm, it remains to determine the components of the right side of Eq. (40).

A. Plane-Symmetric Optical Systems

For plane-symmetric optical designs that are symmetric about the $y-z$ plane, this task is greatly simplified by the fact that the sigma vectors are only along the $\hat{y}$ axis, and therefore every NAT coefficient has no $\hat{x}$ component. However, the polynomial in Eq. (40) does contain various vector operations involving the field coordinate $\vec{H}$ that need to be calculated in order to

determine the vector components of each term:

$$\vec{H} = H_x\hat{x} + H_y\hat{y}, \tag{42}$$

$$\vec{H}^* = -H_x\hat{x} + H_y\hat{y}, \tag{43}$$

$$\vec{H}^2 = 2H_xH_y\hat{x} + \left(-H_x^2 + H_y^2\right)\hat{y}, \tag{44}$$

$$\vec{H}^{2*} = -2H_xH_y\hat{x} + \left(-H_x^2 + H_y^2\right)\hat{y}, \tag{45}$$

$$\vec{H}^3 = H_x\left(3H_y^2 - H_x^2\right)\hat{x} + H_y\left(H_y^2 - 3H_x^2\right)\hat{y}, \tag{46}$$

$$\vec{H}^4 = -4H_xH_y(H_x^2 - H_y^2)\hat{x} + \left(H_x^4 - 6H_x^2H_y^2 + H_y^4\right)\hat{y}. \tag{47}$$

This is all the SVP mathematics that we need to know for a plane-symmetric system. The rest are either inner products or scalar operations. The products between the field coordinates and the NAT coefficients are simplified by the fact that each coefficient simply acts as a scalar since it only has a $\hat{y}$ component.

There are two additional simplifications to the terms in Eq. (40) due to plane symmetry:

$$\vec{B}_{622}^2 = \vec{B}_{622}^{2*} = \left|\vec{B}_{622}^2\right|\hat{y}\,, \tag{48}$$

$$\vec{C}_{622}^3 = \vec{C}_{622}^* = \vec{C}_{622} = \left|\vec{C}_{622}^3\right|\hat{y}\,. \tag{49}$$

Since the conjugate reverses the sign of the $\hat{x}$ component, then the terms $\vec{B}_{622}^2$ and $\vec{B}_{622}^{2*}$ are equal in a plane-symmetric system. Similarly, $\vec{C}_{622}^*$, $\vec{C}_{622}$, and $\vec{C}_{622}^3$ are equal. Therefore, the eighth-order NAT wavefront for a plane-symmetric system has 12 coefficients that determine the field dependence of the Zernike FFD. It is instructive to write this out with the explicit plane-symmetric constraints shown:

$$W_{Z_{5/6}} = \frac{1}{2}\left\{\begin{array}{l}\left[W_{222} + W_{422}H^2 + \boldsymbol{W_{622}H^4} - 2\vec{H}\cdot\left(\left|\vec{A}_{422}\right|\hat{y} + \boldsymbol{2H^2}\left|\vec{A}_{622}\right|\hat{y}\right)\right]\vec{H}^2\ldots\\ +3H^2\left|\vec{B}_{422}\right|\hat{y} + \left|\vec{B}_{622}^2\right|\left(\boldsymbol{6H^4}\,\hat{y} + \vec{H}^4\hat{y}\right)\ldots\\ -2\left(\left|\vec{A}_{222}\right|\hat{y} + H^2\left|\vec{A}_{422}\right|\hat{y} + \boldsymbol{H^4}\left|\vec{A}_{622}\right|\hat{y}\right)\vec{H}\ldots\\ -\left|\vec{C}_{422}^3\right|\hat{y}\,\vec{H}^* - \boldsymbol{4}\left|\vec{C}_{622}^3\right|\hat{y}\vec{H}\left[\boldsymbol{H^2} + \boldsymbol{4}\left(\vec{H}\cdot\hat{y}\right)^2\right]\ldots\\ +\left|\vec{D}_{622}^4\right|\hat{y}\vec{H}^{2*} + \left|\vec{B}_{222}^2\right|\hat{y}\end{array}\right\}\cdot\vec{\rho}^2\,, \tag{50}$$

where we have made the following substitution:

$$\left(H^2\vec{H}^* + \vec{H}^3 + 3H^2\vec{H}\right) = \vec{H}\left[H^2 + 4\left(\vec{H}\cdot\hat{y}\right)^2\right]\,. \tag{51}$$

There are terms in Eq. (50) that contain a SVP operation with the unit vector $\hat{y}$. Any SVP with the unit vector $\hat{y}$ can be simplified with the following identity for any vector $\vec{A} = |\vec{A}|\hat{y}$:

$$\vec{A}\hat{y} = \vec{A}\,. \tag{52}$$

Table 1. Field Dependence of Z5 and Z6 for a $y-z$ Plane-Symmetric System, Broken Down into Each NAT Term and Listed in Ascending Wavefront Expansion Order

NAT Coefficient	Z_5 Field Dependence	Z_6 Field Dependence
W_{222}	$(H_y^2 - H_x^2)$	$2H_xH_y$
$\lvert\vec{A}_{222}\rvert$	$-2H_y$	$-2H_x$
$\lvert\vec{B}_{222}^2\rvert$	1	0
W_{422}	$(H_y^2 - H_x^2)H^2$	$2H_xH_yH^2$
$\lvert\vec{A}_{422}\rvert$	$-4H_y^3$	$-2H_x(H_x^2 + 3H_y^2)$
$\lvert\vec{B}_{422}\rvert$	$3H^2$	0
$\lvert\vec{C}_{422}^3\rvert$	$-H_y$	H_x
W_{622}	$(H_y^2 - H_x^2)H^4$	$2H_xH_yH^4$
$\lvert\vec{A}_{622}\rvert$	$2H_y(H_x^2 - 3H_y^2)H^2$	$-2H_x(H_x^2 + 5H_y^2)H^2$
$\lvert\vec{B}_{622}^2\rvert$	$7H_x^4 + 7H_y^4 + 6H_x^2H_y^2$	$4H_xH_y(H_y^2 - H_x^2)$
$\lvert\vec{C}_{622}^3\rvert$	$-4H_y(H_x^2 + 5H_y^2)$	$-4H_x(H_x^2 + 5H_y^2)$
$\lvert\vec{D}_{622}^4\rvert$	$(H_y^2 - H_x^2)$	$-2H_xH_y$

Therefore, the plane-symmetric NAT wavefront becomes

$$W_{Z_{5/6}} = \frac{1}{2}\left\{\begin{array}{l}\left[W_{222} + W_{422}H^2 + \boldsymbol{W_{622}H^4}\right]\vec{H}^2\ldots\\ +3H^2\left|\vec{B}_{422}\right|\hat{y} + \left|\vec{B}_{622}^2\right|\left(\boldsymbol{6H^4}\,\hat{y} + \vec{H}^4\right)\ldots\\ -2\left|\vec{A}_{222}\right|\vec{H} - 2\left|\vec{A}_{422}\right|\left[H^2\vec{H} + \left(\vec{H}\cdot\hat{y}\right)\vec{H}^2\right]\ldots\\ \boldsymbol{-2\left|\vec{A}_{622}\right|H^2\left[H^2\vec{H} + 2\left(\vec{H}\cdot\hat{y}\right)\vec{H}^2\right]}\ldots\\ -\left|\vec{C}_{422}^3\right|\vec{H}^* \boldsymbol{-4\left|\vec{C}_{622}^3\right|\vec{H}\left[H^2 + 4\left(\vec{H}\cdot\hat{y}\right)^2\right]}\ldots\\ \boldsymbol{+}\left|\vec{D}_{622}^4\right|\vec{H}^{2*} + \left|\vec{B}_{222}^2\right|\hat{y}\end{array}\right\}\cdot\vec{\rho}^2\,. \tag{53}$$

Now each term can be separated into its $\hat{x}$ and $\hat{y}$ components to obtain the contributions to the Z_6 and Z_5 FFDs, respectively. The field dependence of the Z_5 and Z_6 polynomials separated into each NAT term is shown in Table 1.

The FFD of each NAT term from Table 1 is shown in Fig. 1. The Z5 and Z6 components are combined and represented by a line marker. The magnitude and orientation of the line at each field point are given by Eq. (54). The line magnitude represents the peak-to-valley magnitude of the Z5/6 wavefront error, and the angle represents the orientation of the peaks of the wavefront error relative to the coordinate system of the image plane:

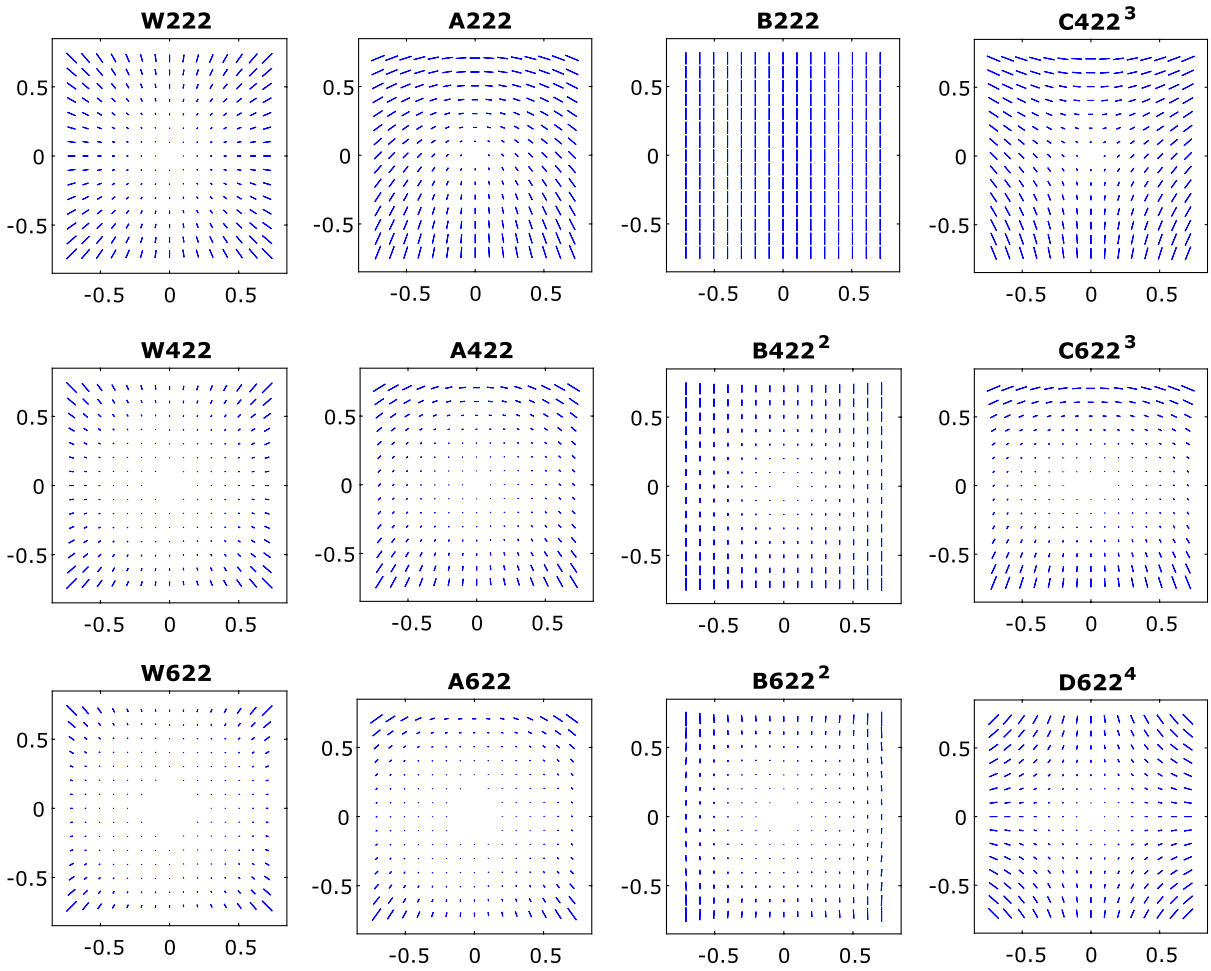

Fig. 1. Zernike Z5/6 full-field display of each NAT plane-symmetric field dependence.

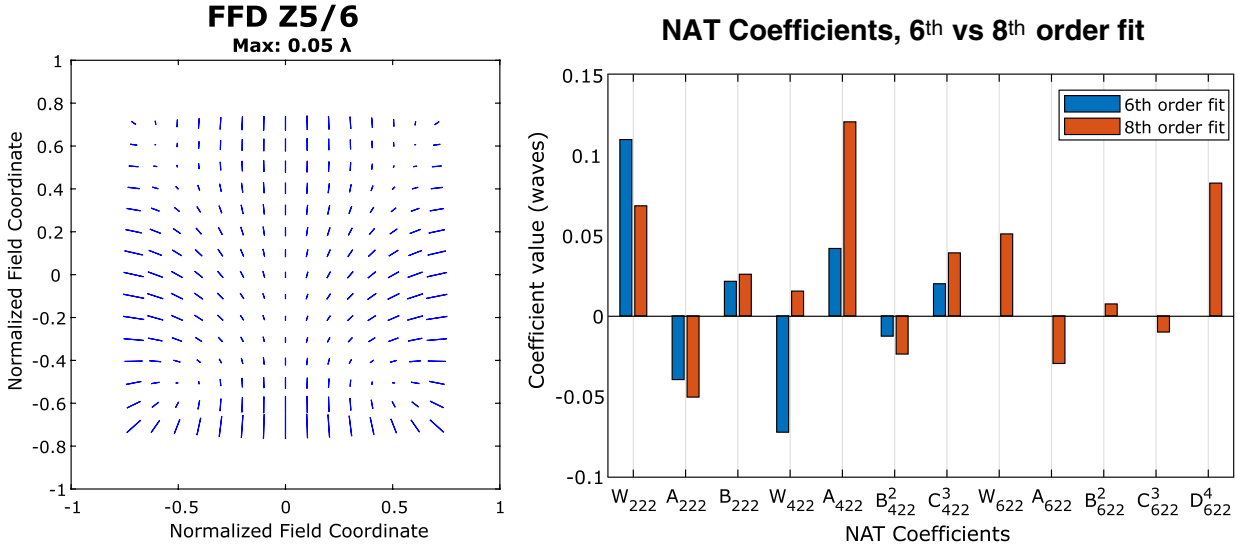

(a) (b)

Fig. 2. (a) Zernike Z5/6 FFD of an optimized optical design with high-order aberration terms. (b) Comparison of the NAT coefficient estimation using the sixth-order versus the eighth-order NAT astigmatism polynomial of the FFD data in (a).

$$|Z_{5/6}| = \sqrt{z_6^2 + z_5^2},$$

$$\phi_{Z5/6} = \frac{1}{2}\tan^{-1}\left(\frac{z_6}{z_5}\right). \tag{54}$$

The expansion to the eighth order yields different and more accurate estimations of the NAT coefficients, especially when higher-order terms start to dominate the Z5/6 astigmatism FFD. Figure 2(a) shows the astigmatism FFD characteristic of a well-corrected freeform three-mirror telescope. It is difficult to ascertain the constituent field-dependent terms just by visually inspecting the FFD. Figure 2(b) shows the NAT coefficients estimated by fitting the FFD data with the NAT astigmatism polynomial for up to sixth-order terms (blue) and up to eighth-order terms (red). In this case, we see significant differences in the estimate of the NAT coefficients between the two fits due to the relatively high magnitude of the higher-order terms.

4. ESTIMATING REQUIRED FREEFORM SURFACE DEPARTURE

The ATFS and later the work of Bauer *et al.* provided a framework and design method for freeform mirror designs [3,5]. This design method systematically introduces each Zernike polynomial surface term into a specific surface in the design to correct specific aberrations based on ATFS. Comparison of this systematic, aberration-based approach to a numerical optimization method that is blind to the aberrations can be found in Takaki *et al.* [23]. We can use the methods exposed in Bauer *et al.* to theorize a calculus that allows us to quantitatively analyze a given design. The analysis we present here involves determining each surface's effect on a given set of NAT aberrations. We have completed this analysis for three main Zernike surface shapes: Z5 (astigmatism), Z8 (coma), and Z11 (trefoil).

A. Zernike Astigmatism Shape (Z5)

From previous work, we know that adding a Z5 shape to any surface in the design produces field-constant astigmatism ($\vec{B}^2_{222}$). The overall field-constant astigmatism is given by [Eq. (14) from [3]]

$$\vec{B}^2_{222} = {}_G\vec{B}^2_{222} + \sum_{j=1}^{n} {}_{FF}\vec{B}^2_{222,j}. \tag{55}$$

Here ${}_G\vec{B}^2_{222}$ is the field-constant astigmatism from the geometry of the spherical surfaces and is proportional to the square of the sigma vectors of the tilted surfaces ($\vec{\sigma}_j^{\,2}$). Similarly, a Z5 shape on a given surface j gives ${}_{FF}\vec{B}^2_{222,j}$, the field-constant astigmatism term for that surface. ${}_{FF}\vec{B}^2_{222,j}$ is proportional to the Z5/6 surface coefficients for that surface. In the plane-symmetric case, it is proportional to Z5:

$${}_{FF}B^2_{222,j} \equiv B^{\alpha}_{222,j} Z_{5,j}. \tag{56}$$

Here we have introduced a new notation using α to denote the proportionality constant $B^{\alpha}_{222,j}$ between a given Zernike surface shape coefficient $Z_{5,j}$ and a given NAT coefficient for a surface j. We have also dropped the vector notation for the plane-symmetric case for the sake of simplicity. We see from Eqs. (55) and (56) that to completely correct $\vec{B}^2_{222}$ using a given surface j, we set the surface coefficient $Z_{5,j}$ equal to the total field-constant astigmatism divided by its proportionality constant:

$$Z_{5,j}\big|_{B_{222}=0} = -\frac{{}_G B^2_{222}}{B^{\alpha}_{222,j}}. \tag{57}$$

Equation (57) assumes there is a linear relationship between the Z5 surface shape coefficient of a given surface and the NAT coefficient for field-constant astigmatism. We implicitly assume this relationship based on [3]. The relationship has been validated by the design methods shown in [5,16–18].

B. Zernike Coma Shape (Z8)

Once field-constant astigmatism is removed, often the next largest aberration is field-constant coma ($\vec{A}_{131}$) together with field-linear, field-asymmetric astigmatism ($\vec{A}_{222}$). From [3], we know that adding a Z8 shape to an optical surface produces both field-linear, field-asymmetric astigmatism ($\vec{A}_{222}$) and field-constant coma ($\vec{A}_{131}$) terms as well as field-linear defocus ($\vec{A}_{220M}$), also known as focal plane tilt [3]:

$$\vec{A}_{131} = {}_G\vec{A}_{131} - \sum_{j=1}^{n} {}_{FF}\vec{A}_{131,j}, \tag{58}$$

$$\vec{A}_{222} = {}_G\vec{A}_{222} - \sum_{j=1}^{n} \left(\frac{\bar{y}}{y}\right) {}_{FF}\vec{A}_{131,j}, \tag{59}$$

$$\vec{A}_{220M} = {}_G\vec{A}_{220M} - \sum_{j=1}^{n} \left(\frac{\bar{y}}{y}\right) {}_{FF}\vec{A}_{131,j}. \tag{60}$$

We can again write the proportionality constants for these terms relative to the surface coefficient Z8 (and again dropping the vector notation):

$$-{}_{FF}A_{131,j} \equiv A^{\alpha}_{131,j} z_{8,j}, \tag{61}$$

$$-\left(\frac{\bar{y}}{y}\right) {}_{FF}A_{131,j} \equiv A^{\alpha}_{222,j} z_{8,j}. \tag{62}$$

Here we will show an example of how to correct field-asymmetric, field-linear astigmatism ($\vec{A}_{222}$) and field-constant coma ($\vec{A}_{131}$) using two surfaces. The residual blur from the focal plane tilt can be corrected by tilting the physical image plane, so its proportionality constant has not been defined here.

Section 3.A showed how to determine A_{222}. Field-constant coma A_{131} is equivalent to the Zernike coma (Z8) coefficient at the central field point, e.g., $(H_x, H_y) = (0, 0)$. To simultaneously correct both $\vec{A}_{131}$ and $\vec{A}_{222}$, we know from [5] that we need two freeform surfaces with a Z8 surface shape. The total magnitude of these two aberrations in a system with two surfaces using a Z8 shape is given by combining Eqs. (58) and (59) with Eqs. (61) and (62):

$$A_{131} = A_{131,G} + A^{\alpha}_{131,a} z_{8,a} + A^{\alpha}_{131,b} z_{8,b} \equiv 0, \tag{63}$$

$$A_{222} = A_{222,G} + A^{\alpha}_{222,a} z_{8,a} + A^{\alpha}_{222,b} z_{8,b} \equiv 0. \tag{64}$$

Solving this system of equations for the required surface coefficients gives

$$\begin{aligned} z_{8,a}\big|_{A_{131},A_{222}=0} &= \frac{-A^{\alpha}_{222,b}\,({}_G A_{131}) + A^{\alpha}_{131,b}\,({}_G A_{222})}{A^{\alpha}_{131,a}A^{\alpha}_{222,b} - A^{\alpha}_{131,b}A^{\alpha}_{222,a}}, \\ z_{8,b}\big|_{A_{131},A_{222}=0} &= \frac{A^{\alpha}_{222,a}\,({}_G A_{131}) - A^{\alpha}_{131,a}\,({}_G A_{222})}{A^{\alpha}_{131,a}A^{\alpha}_{222,b} - A^{\alpha}_{131,b}A^{\alpha}_{222,a}}. \end{aligned} \tag{65}$$

It is convenient to define the ratio of A_{131} to A_{222} proportionality constants for each surface and for the ratio of the overall aberrations:

$$\begin{aligned} R_{Z_8,j} &\equiv \frac{A^{\alpha}_{222,j}}{A^{\alpha}_{131,j}}, \\ R_{Z_8,\mathrm{sys}} &\equiv \frac{{}_G A_{222}}{{}_G A_{131}}. \end{aligned} \tag{66}$$

Rewriting Eq. (65), we get the solution in terms of these ratios:

$$\begin{aligned} z_{8,a}\big|_{A_{131},A_{222}=0} &= -\frac{({}_G A_{131})}{A^{\alpha}_{131,a}} \frac{\left(R_{Z_8,\mathrm{sys}} - R_{Z_8,b}\right)}{\left(R_{Z_8,a} - R_{Z_8,b}\right)}, \\ z_{8,b}\big|_{A_{131},A_{222}=0} &= \frac{({}_G A_{131})}{A^{\alpha}_{131,b}} \frac{\left(R_{Z_8,\mathrm{sys}} - R_{Z_8,a}\right)}{\left(R_{Z_8,a} - R_{Z_8,b}\right)}. \end{aligned} \tag{67}$$

One way to understand Eq. (67) is to imagine incrementally changing the coefficient for a given surface, say $z_{8,a}$, until the ratio of the total aberrations A_{222}/A_{131} is equal to the ratio of the proportionality constants for the *other* surface coefficient $z_{8,b}$. Then we can increment that surface coefficient $z_{8,b}$ until both aberrations vanish. Equation (67) accomplishes this task by solving the system of equations directly.

C. Zernike Trefoil Shape (Z11)

After correcting $\vec{B}_{222}$, $\vec{A}_{222}$, $\vec{A}_{131}$, often the next largest non-symmetric aberrations are field-constant elliptical coma $\vec{C}^{3}_{333}$ and field-linear, field-conjugate astigmatism $\vec{C}^{3}_{422}$. From [3] and [5], we know that a Zernike trefoil (Z11) shape on a surface produces these aberrations, and therefore we can use a similar procedure as in Section 4.B to obtain the required Z11 surface coefficients for two surfaces to simultaneously correct $\vec{C}^{3}_{333}$ and $\vec{C}^{3}_{422}$:

$$\begin{aligned} z_{11,a}\big|_{C^3_{333},C^3_{422}=0} &= -\frac{\left(C^{3}_{333,G}\right)}{C^{3,\alpha}_{333,a}} \frac{\left(R_{Z_{11},\mathrm{sys}} - R_{Z_{11},b}\right)}{\left(R_{Z_{11},a} - R_{Z_{11},b}\right)}, \\ z_{11,b}\big|_{C^3_{333},C^3_{422}=0} &= \frac{\left(C^{3}_{333,G}\right)}{C^{3,\alpha}_{333,b}} \frac{\left(R_{Z_{11},\mathrm{sys}} - R_{Z_{11},a}\right)}{\left(R_{Z_{11},a} - R_{Z_{11},b}\right)}. \end{aligned} \tag{68}$$

5. DESIGN EXAMPLE

The eighth-order NAT expansion can be used to estimate the required freeform departure to correct various NAT aberrations for a given freeform design, and, significantly, this is done without ray-trace optimization. Using the field dependences in Table 1, programs were implemented in CODE V to compute the NAT coefficients given the Z_5 and Z_6 wavefront coefficients at field points throughout the FOV. To estimate the NAT coefficients, the CODE V algorithm uses singular value decomposition to solve the system of equations given by Table 1 with the input of the Z_5 and Z_6 FFD data. The Z_5 and Z_6 data was collected by fitting the wavefront at the exit pupil without ray aiming with the FRINGE Zernike polynomials up to Z37 (see [24] for polynomial details) for each field point, as is done in the FFD plots in CODE V. The wavefront is sampled by computing the optical path difference of 58×58 rays traced across the pupil (the default in CODE V). As an example, we show the use of this method using a design from the literature.

The example design is a freeform three-mirror compact (TMC) design used in [5]. This design is the classic TMC geometry made more compact using freeform surfaces. It uses a positive-negative-positive optical power distribution on the mirrors, and has the stop at the primary mirror. The design uses a 200 mm entrance pupil diameter working at F/3 with a $4° \times 4°$ square field of view. All analyses are done at a wavelength of 587 nm. A cross-sectional layout of the design stripped of the freeform terms, leaving only the base spherical surfaces, is shown in Fig. 3.

The process of adding freeform shapes to the surfaces starts with an all-spherical design. We started with the final design from [5] and removed the freeform terms, leaving only the tilted spherical surfaces. Often, designing unobscured three-mirror freeform telescopes requires re-optimizing the radii or adjusting the first-order layout as described in [5]. However, the purpose of the techniques described in this work is to provide a method to estimate the required freeform departure to correct a given aberration and not to re-optimize the first-order layout. The first step towards adding freeform is to examine the FFDs and the relevant NAT aberration coefficients. The FFDs for the design with only spherical surfaces are shown in Fig. 4. Select NAT aberration coefficients derived from these FFDs are shown in Fig. 5.

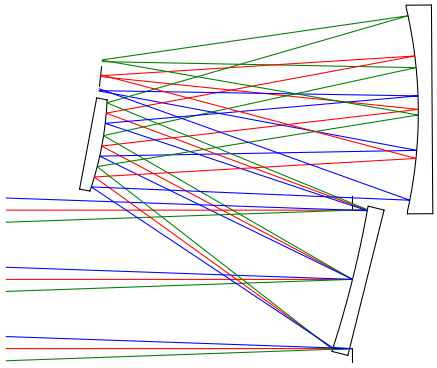

Fig. 3. Layout of the example TMC design from Bauer *et al.* with freeform surface terms removed, leaving only the base spherical surfaces.

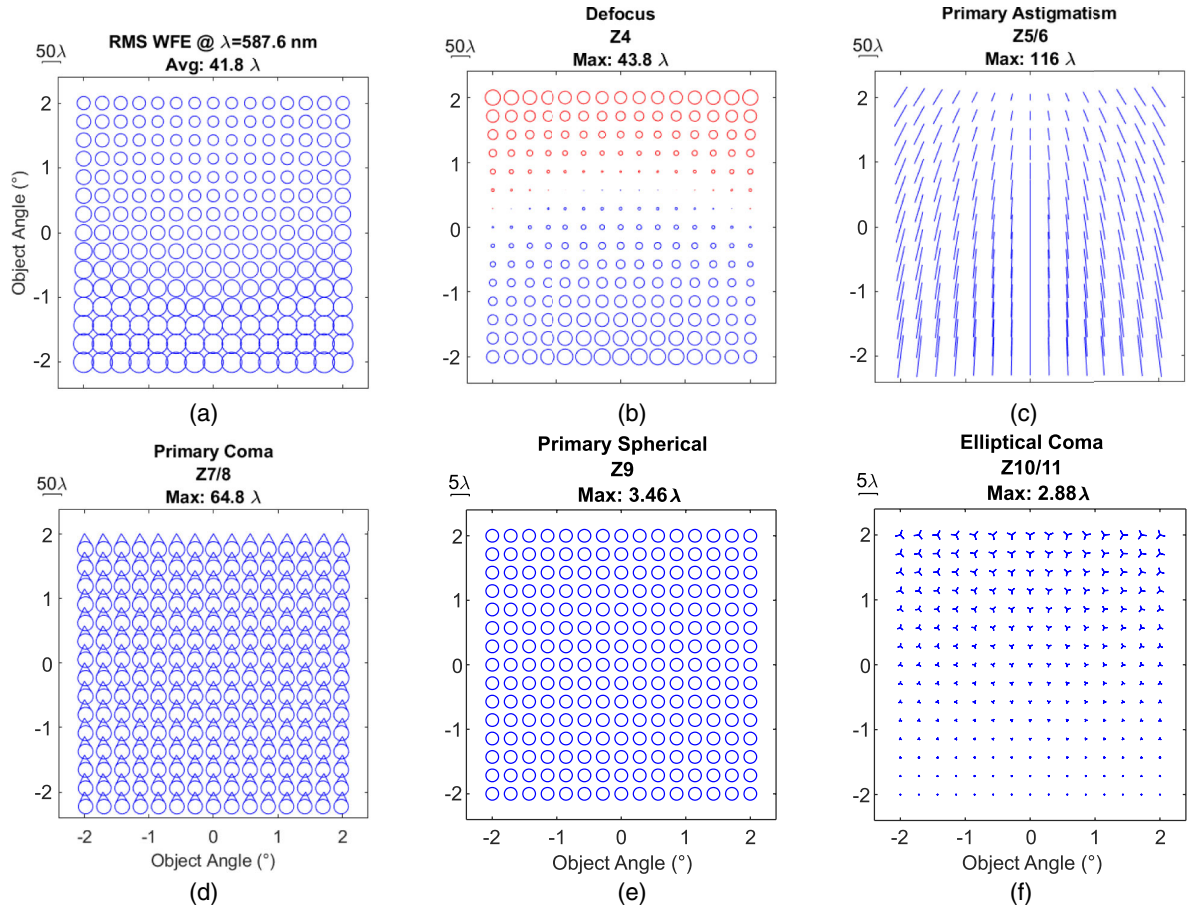

Fig. 4. Full-field displays for the design with all-spherical surfaces. Units are waves at 532 nm: (a) RMS wavefront error (WFE); (b) defocus (Z4); (c) astigmatism, Z5/6; (d) coma, Z7/8; (e) spherical, Z9; (f) elliptical coma, Z10/11.

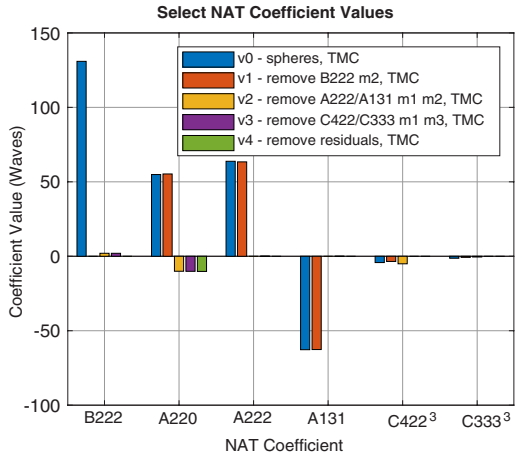

Fig. 5. Selected NAT coefficients related to the Zernike surface terms Z5 (astigmatism), Z8 (coma), and Z11 (trefoil, or elliptical coma) shown at each step.

From this point, we would like to estimate the required coefficients to remove, in order, B_{222}, A_{222}/A_{131}, and C_{422}/C_{333} using Eqs. (57), (67), and (68), respectively. However, first we must calculate the respective aberration ratios and therefore the respective proportionality constants. One way to calculate these values is to use the relations given by Fuerschbach *et al.* that relate the Zernike surface shape coefficients to the NAT aberration terms [3]. In practice, however, these relationships are difficult to implement and produce a small inaccuracy because they do not consider the induced aberrations of the system. In this example, we have opted to use a differential technique to estimate the proportionality constants. To do so, the NAT coefficients are first estimated. Then a single Zernike surface coefficient is changed by a small amount, and the NAT coefficients are estimated again. This technique has the advantage of including any induced aberration effects. Additionally, it directly relates the coefficient in the design software with the aberration, regardless of the Zernike normalization radius.

A. Correcting B_{222}^2

From Fig. 4 we can see that the dominant aberration is primarily field-constant astigmatism, so we begin by correcting field-constant astigmatism as in Bauer *et al.* [5]. However, here we make use of our ability to estimate B_{222}. Table 2 shows the result of two iterations of this process. Using Eq. (57), we can predict that adding −23.4 μm of Z5 to the stop surface will remove this field-constant astigmatism, and after it is added, we see that the B_{222} term is reduced by a factor of 7e4. A second iteration of re-estimating the proportionality constant and

Table 2. B_{222} Removal Process with Two Iterations

	Iteration 1	Iteration 2
Starting B_{222} Value (waves)	130.911	−0.018
$B^{\alpha}_{222,\mathrm{M1}}$ (waves/micrometers)	5.59	5.63
$Z_{5,\mathrm{M1}}\vert_{B_{222}=0}$ (micrometers)	−23.4261	−23.4229
Final B_{222} Value (waves)	−0.018	8.9e-008

adjusting the surface coefficient accordingly further reduces B_{222} to negligible levels. This iteration process can be used as an aberration-based optimization routine. The resulting Z5 FFD is shown in Fig. 7(b).

Note that the proportionality constant for a given coefficient will depend on the normalization radius. In this work, each freeform surface has a normalization radius equal to the semi-diameter of the clear aperture for that surface. This choice of normalization radius allows the coefficients to be normalized to the entire used aperture of the surface and ensures that rays will not miss the surface. Choosing the normalization radius to be the semi-diameter of the central field footprint may be more convenient for NAT but does not always guarantee an error-free ray trace.

B. Correcting A_{222} and A_{131} Simultaneously

Once B_{222} is removed, A_{222} and A_{131} are the next largest aberrations as can be seen in Fig. 5. Using Eq. (67), we can estimate the coefficients required for any pair of surfaces, e.g., M1 and M2 or M1 and M3, etc. Examining the ratios in Fig. 6(a) can help determine which two surfaces will be most effective in removing these two aberrations. The "effectiveness" is based on the required departure that each surface needs to remove these two aberrations. In this particular example, we see that the Z8 ratio for the system as whole is smaller than the ratios for M2 and M3. M1, the stop surface, has a ratio that is zero, since a Z8 shape at the stop only produces field-constant coma in the wavefront. Therefore, just by looking at the ratios, we know that, by adding some amount of Z8 to the stop surface, we can increase the magnitude of the overall system ratio until it is equal to the ratio of M2. From there, adding any amount of M2 will either increase or decrease both A_{222} and A_{131} by the same relative amount, and we can then drive both terms to zero. The same could be done for M2 and M3, but using M2 to make the system ratio equal to the M3 ratio would require more surface aberrations to be added and therefore more surface departure. This analysis can be summarized by Table 3. To reduce the overall freeform departure required, we can choose the combination of surfaces that corrects the aberrations with the least departure based on the values in Table 3. In the case of this design, M1 and M2 require the least departure. Using M1 and M2 to remove A_{222} and A_{131}, we can see the resulting Z5/6 FFD in Fig. 7(c) and the resulting Z7/8 FFD in Fig. 8(c).

C. Correcting $\vec{C}^{3}_{333}$ and $\vec{C}^{3}_{422}$ Simultaneously with a Z11 Shape on Two Mirrors

The relevant proportionality constants and ratios can be similarly analyzed for a Z11 shape on two surfaces. The relative ratios for each mirror and for the overall aberrations are shown in Fig. 6(b). In the case of a Z11 shape, both non-stop surfaces have positive ratios along with the overall system ratio. The M3 ratio is closest to the overall aberration ratio.

Using a Z11 shape on M1 will add only field-constant elliptical coma ($\vec{C}^{3}_{333}$), which will lower the $R_{Z_{11},\mathrm{sys}}$ ratio. If the correct amount is added, the $R_{Z_{11},\mathrm{sys}}$ ratio will be equal to the M3 ratio. Then, adding a Z11 shape on M3 will reduce both C_{333} and C_{422} in the right proportions to simultaneously drive them both to zero. We could instead add even more $\vec{C}^{3}_{333}$ to lower the overall $R_{Z_{11},\mathrm{sys}}$ ratio further to equal the M2 ratio, but this would require adding more surface departure and more aberrations than in the M1–M3 case. Similarly, the combination of M2 and M3 could be used. However, this would be even less efficient

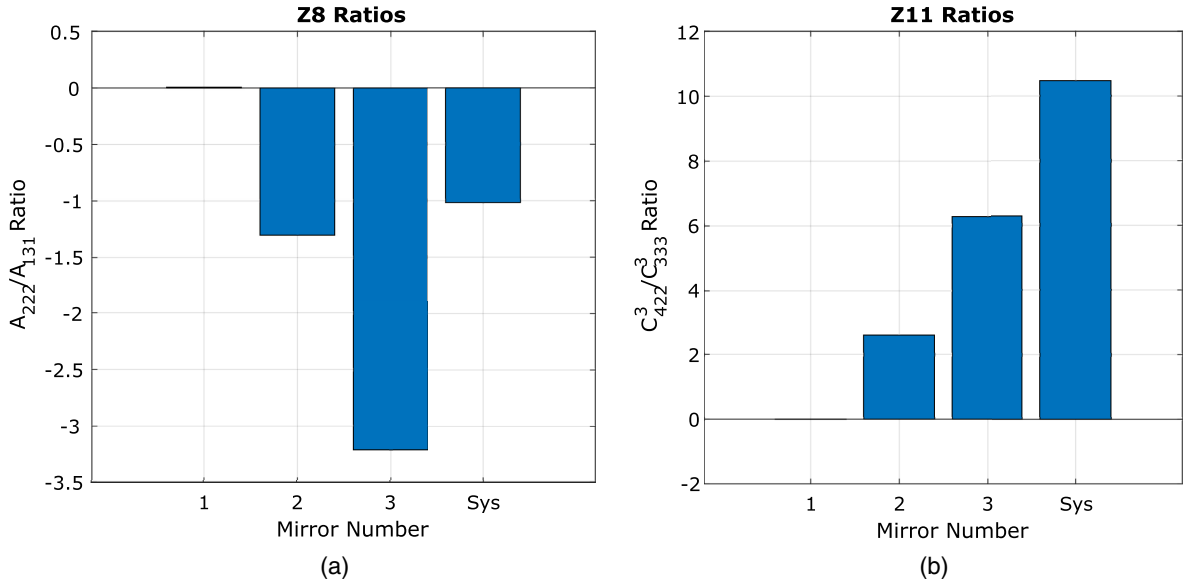

Fig. 6. (a) Ratios of A_{222} and A_{131} from adding a Z8 shape onto each mirror and for the overall aberrations seen in Fig. 5. (b) Ratios of C_{422} and C_{333} from adding a Z11 shape onto each mirror and for the overall aberrations seen in Fig. 5.

Table 3. A_{222}/A_{131} Ratio for Each Pair of Surfaces and the Resulting Predicted Surface Coefficients

Overall Z8 Aberrations (Waves)		Z8 Proportionality Constants and Ratio Values (Waves/Micrometers)	M1	M2	M3
${}_GA_{222}$	63.34	$A^{\alpha}_{222,j}$	−0.02141	−1.649	1.491
${}_GA_{131}$	−62.64	$A^{\alpha}_{131,j}$	−3.019	1.267	−0.4658
Ratio	−1.01	Ratio	0.00709	−1.30	−3.20
		Predicted Surface Coefficients (Micrometers)			
			M1	**M2**	**M3**
		M1 + M2	4.59	−38.48	–
		M2 + M3	–	−56.95	−20.50
		M1 + M3	14.16	–	42.69

than either of the other two cases, since more departure and aberrations would need to be added using M2 to change the overall aberration ratio to the ratio of M3. Therefore, we proceed with M1 and M3 and use Eq. (68) to remove C_{422} and C_{333} simultaneously. The resulting Z5/6 FFD is shown in Fig. 7(d), and the resulting Zernike elliptical coma (Z10/11) is shown in Fig. 9(d). In this case, only a single iteration was necessary to reduce both C_{422} and C_{333} below 1e-7 waves.

D. Discussion

Examining Figs. 5 and 7(d), we see that there is some residual field-constant astigmatism (B_{222}) that has been accrued in the A_{222}/A_{131} correction step, even though it was already corrected using a Z5 shape at M1, as indicated by the small but non-zero value of Z5/6 seen at the center of the FFD in Fig. 7(c). The exact cause of this is not obvious by considering only ATFS and NAT alone, but induced aberrations are likely to blame [25,26]. Once we begin adding many waves of, for instance, Z8 departure onto surfaces that have non-collimated beam footprints as in Section 5.B, the assumptions that allow us to ignore induced aberrations begin to break down. Additionally, the beam footprint on any given surface is not always circular but is often elliptical, causing a deviation from the pupil and field dependence of each freeform term shown by the ATFS [4]. The amount of aberration added by a freeform surface also depends not only on the sag of the surface but also on the angle of incidence of the rays. Ray bundles from different field points may strike a surface at different angles of incidence and therefore pick up a different amount of aberration. These sources of error contribute to the deviation from linearity of the surface coefficient prediction. However, applying another iteration of each step removes the small residual B_{222}, A_{222}/A_{131}, and C_{422}/C_{333} aberrations. The resulting FFDs are shown in Figs. 7(e), 8(e), and 9(e). Additionally, Fig. 5 shows the relevant NAT coefficients at each step and how each step affects the residual aberrations of the others.

Regarding the collection of the Z_5 and Z_6 FFD data, note that in general the accuracy of the wavefront fit depends on the number of rays traced across the pupil. In the example design in this work, we found that the default number of rays in CODE V of 58 × 58 rays across the entrance pupil was sufficient, and increasing the number of rays did not change the wavefront fit results appreciably.

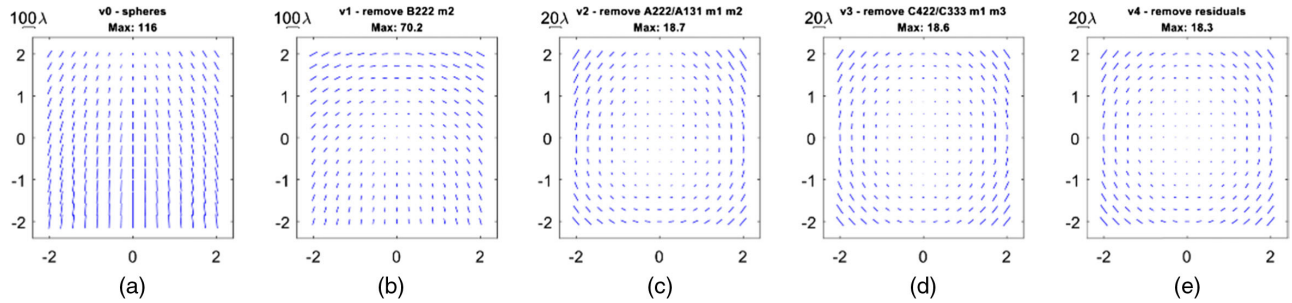

Fig. 7. Astigmatism (Z5/6) FFDs after each step. The axes' units are the object field angle coordinates in degrees. (a) Starting design without any freeform (spheres only); (b) after B_{222} removal; (c) after A_{222}/A_{131} removal; (d) after C_{422}/C_{333} removal; (e) after removing the residuals of each terms through another iteration of each step.

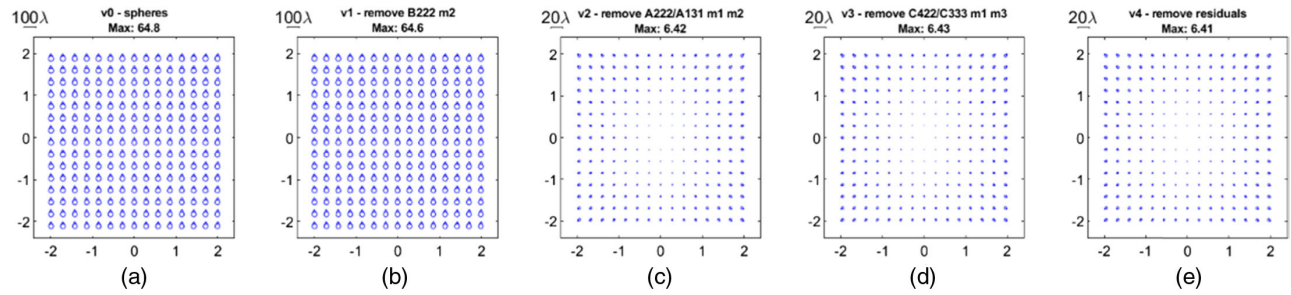

Fig. 8. Zernike Coma (Z7/8) FFDs for each step. The axes' units are the object field angle coordinates in degrees. (a) Starting design without any freeform (spheres only); (b) after B_{222} removal; (c) after A_{222}/A_{131} removal; (d) after C_{422}/C_{333} removal; (e) after removing the residuals through another iteration of each step.

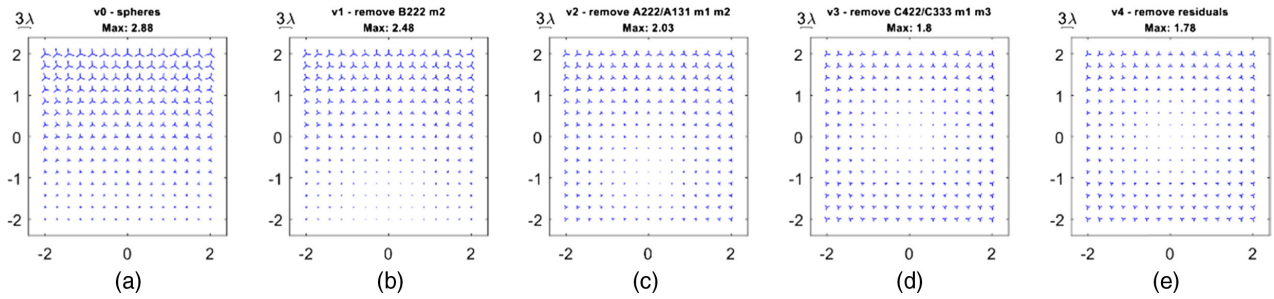

Fig. 9. Zernike Elliptical Coma (Z10/11) for each step. The axes' units are the object field angle coordinates in degrees. (a) Starting design without any freeform (spheres only); (b) after B_{222} removal; (c) after A_{222}/A_{131} removal; (d) after C_{422}/C_{333} removal; (e) after removing the residuals through another iteration of each step.

E. Higher-Order Zernike Surface Coefficients

The ATFS as detailed in [3] includes analysis of higher-order Zernike terms beyond Z10/11. Additionally, previous work detailing a freeform design method that relies on ATFS includes a qualitative analysis of the FFDs for these higher-order Zernike surface shapes [5]. In the present work, we have carried out a quantitative analysis up to Z10/11 surface shapes because shapes with higher orders than this produce more complicated field dependence in Zernike aberration FFDs besides astigmatism (Z5/6). Using similar methods to extend to higher-order FFDs is certainly feasible; it requires analyzing the field dependence of the relevant Zernike aberrations, which is envisioned as future work.

6. CONCLUSION

We have expanded the field dependence of Zernike astigmatism (Z5/6) up to the eighth order in a wavefront by expanding the NAT wavefront up to the eighth order and collecting the terms with new field dependence. We have then shown how to use insights from ATFS to estimate the required Zernike surface coefficients to correct certain NAT terms in plane-symmetric optical systems as a tool for freeform design. The Z5, Z8, and Z11 surface shapes for plane-symmetric optical systems have been analyzed and methods to predict their required coefficients given. As an example, a three-mirror freeform design from previous work was analyzed using these methods, and the method was shown to be effective at predicting the required surface coefficients and correcting the intended aberrations.

APPENDIX A

Below are some useful vector identities involving the SVP for deriving the equations in Section 2.A. Equations (A1) and (A2) are reproduced from [11]:

$$2\left(\vec{A}\cdot\vec{B}\right)\left(\vec{A}\vec{B}\cdot\vec{C}^2\right)=\left(\vec{A}\cdot\vec{A}\right)\left(\vec{B}^2\cdot\vec{C}^2\right)+\left(\vec{B}\cdot\vec{B}\right)\left(\vec{A}^2\cdot\vec{C}^2\right), \tag{A1}$$

$$2\left(\vec{A}\cdot\vec{B}\right)\left(\vec{A}^2\cdot\vec{C}^2\right)=\left(\vec{A}\cdot\vec{A}\right)\left(\vec{A}\vec{B}\cdot\vec{C}^2\right)+\vec{A}^3\cdot\vec{B}\vec{C}^2. \tag{A2}$$

Equation (A3) can be derived from Eqs. (5) and (A1):

$$2\left(\vec{A}^2\cdot\vec{B}^2\right)\left(\vec{A}\vec{B}\cdot\vec{C}^2\right)=\left(\vec{A}\cdot\vec{A}\right)\left(\vec{B}^3\cdot\vec{A}\vec{C}^2\right)+\left(\vec{B}\cdot\vec{B}\right)\left(\vec{A}^3\cdot\vec{B}\vec{C}^2\right). \tag{A3}$$

The following equations follow from the identities in Eqs. (5) and (A1)–(A3). They are listed in here the order in which they are used in Section 2.A:

$$\left(\vec{H}\cdot\vec{\sigma}_j\right)\left[\left(\vec{H}\vec{\sigma}_j\right)\cdot\vec{\rho}^2\right]=\frac{1}{2}H^2\vec{\sigma}_j^2\cdot\vec{\rho}^2+\frac{1}{2}\sigma_j^2\vec{H}^2\cdot\vec{\rho}^2, \tag{A4}$$

$$\left(\vec{H}^2\cdot\vec{\sigma}_j^2\right)\left(\vec{H}^2\cdot\vec{\rho}^2\right)=\frac{1}{2}H^4\vec{\sigma}_j^2\cdot\vec{\rho}^2+\frac{1}{2}\vec{H}^4\left(\vec{\sigma}_j^*\right)^2\cdot\vec{\rho}^2, \tag{A5}$$

$$2\left(\vec{H}\cdot\vec{\sigma}_j\right)\left(\vec{\sigma}_j^2\cdot\vec{\rho}^2\right)=\sigma_j^2\vec{\sigma}_j\vec{H}\cdot\vec{\rho}^2+\vec{\sigma}_j^3\cdot\vec{H}\vec{\rho}^2=\sigma_j^2\vec{\sigma}_j\vec{H}\cdot\vec{\rho}^2+\vec{\sigma}_j^3\vec{H}^*\cdot\vec{\rho}^2, \tag{A6}$$

$$2\left(\vec{H}^2\cdot\vec{\sigma}_j^2\right)\left(\vec{H}\vec{\sigma}_j\cdot\vec{\rho}^2\right)=H^2\vec{\sigma}_j^3\cdot\vec{H}\vec{\rho}^2+\sigma_j^2\vec{H}^3\cdot\vec{\sigma}_j\vec{\rho}^2=H^2\vec{H}^*\vec{\sigma}_j^3\cdot\vec{\rho}^2+\sigma_j^2\vec{\sigma}^*\vec{H}^3\cdot\vec{\rho}^2, \tag{A7}$$

$$2\sigma_j^2\left(\vec{H}\cdot\vec{\sigma}_j\right)\left(\vec{\sigma}_j^2\cdot\vec{\rho}^2\right)=H^2\sigma_j^2\left(\vec{\sigma}_j\vec{H}\cdot\vec{\rho}^2\right)+H^2\left(\vec{H}^*\vec{\sigma}_j^3\cdot\vec{\rho}^2\right), \tag{A8}$$

$$2\sigma_j^2\left(\vec{H}\cdot\vec{\sigma}_j\right)\left(\vec{H}^2\cdot\vec{\rho}^2\right)=H^2\sigma_j^2\left(\vec{\sigma}_j\vec{H}\cdot\vec{\rho}^2\right)+\sigma_j^2\left(\vec{\sigma}_j^*\vec{H}^3\cdot\vec{\rho}^2\right), \tag{A9}$$

$$\left(\vec{H}^2\cdot\vec{\sigma}_j^2\right)\left(\vec{\sigma}_j^2\cdot\vec{\rho}^2\right)=\frac{1}{2}\left(\vec{\sigma}_j^2\cdot\vec{\sigma}_j^2\right)\left(\vec{H}^2\cdot\vec{\rho}^2\right)+\frac{1}{2}\vec{\sigma}_j^4\cdot\vec{H}^2\vec{\rho}^2=\frac{1}{2}\sigma_j^4\left(\vec{H}^2\cdot\vec{\rho}^2\right)+\frac{1}{2}\left(\vec{\sigma}_j^4\vec{H}^{2*}\cdot\vec{\rho}^2\right), \tag{A10}$$

$$4\sigma_j^2\left(\vec{H}\cdot\vec{\sigma}_j\right)\left(\vec{H}\vec{\sigma}_j\cdot\vec{\rho}^2\right)=2\sigma_j^2H^2\left(\vec{\sigma}_j^2\cdot\vec{\rho}^2\right)+2\sigma_j^4\left(\vec{H}^2\cdot\vec{\rho}^2\right),\quad\textbf{(A11)}$$

$$2\sigma_j^2\left(\vec{H}\cdot\vec{\sigma}_j\right)\left(\vec{\sigma}_j^2\cdot\vec{\rho}^2\right)=\sigma_j^4\left(\vec{\sigma}_j\vec{H}\cdot\vec{\rho}^2\right)+\sigma_j^2\left(\vec{\sigma}_j^3\vec{H}^*\cdot\vec{\rho}^2\right).\quad\textbf{(A12)}$$

Equations (A5) and (A10) follow from Eq. (5). Equations (A4) and (A11) follow from Eq. (A1). Equations (A6), (A8), (A9), and (A12) follow from Eq. (A2). Equation (A7) follows from Eq. (A3).

Funding. National Science Foundation (IIP-1338877, IIP-1338898, IIP-1822026, IIP-1822049); National Nuclear Security Administration (DE-NA0001944).

Acknowledgment. This research was supported by the National Science Foundation I/UCRC Center for Freeform Optics and the National Nuclear Security Administration through the Frank J. Horton Graduate Research Fellowship awarded by the Laboratory for Laser Energetics at the University of Rochester.

Disclosures. The authors declare no conflicts of interest.

REFERENCES

1. R. V. Shack and K. Thompson, "Influence of alignment errors of a telescope system on its aberration field," in *Optical Alignment I* (International Society for Optics and Photonics, 1980), Vol. **0251**, pp. 146–153.
2. K. P. Thompson, "Description of the third-order optical aberrations of near-circular pupil optical systems without symmetry," J. Opt. Soc. Am. A **22**, 1389–1401 (2005).
3. K. Fuerschbach, J. P. Rolland, and K. P. Thompson, "Theory of aberration fields for general optical systems with freeform surfaces," Opt. Express **22**, 26585–26606 (2014).
4. T. Yang, D. Cheng, and Y. Wang, "Aberration analysis for freeform surface terms overlay on general decentered and tilted optical surfaces," Opt. Express **26**, 7751–7770 (2018).
5. A. Bauer, E. M. Schiesser, and J. P. Rolland, "Starting geometry creation and design method for freeform optics," Nat. Commun. **9**, 1756 (2018).
6. D. Reshidko and J. Sasian, "Method for the design of nonaxially symmetric optical systems using free-form surfaces," Opt. Eng. **57**, 101704 (2018).
7. J. R. Rogers, "Techniques and tools for obtaining symmetrical performance from tilted-component systems," Opt. Eng. **39**, 1776–1787 (2000).
8. K. P. Thompson and J. P. Rolland, "A page from "the drawer": How Roland Shack opened the door to the aberration theory of freeform optics," Proc. SPIE **9186**, 91860A (2014).
9. H. H. Hopkins, *Wave Theory of Aberrations* (Clarendon, 1950).
10. R. A. Buchroeder, "Tilted component optical systems," Ph.D. dissertation (University of Arizona, 1976).
11. K. P. Thompson, "Aberration fields in tilted and decentered optical systems," Ph.D. dissertation (University of Arizona, 1980).
12. K. P. Thompson, T. Schmid, O. Cakmakci, and J. P. Rolland, "Real-ray-based method for locating individual surface aberration field centers in imaging optical systems without rotational symmetry," J. Opt. Soc. Am. A **26**, 1503–1517 (2009).
13. K. P. Thompson, "Multinodal fifth-order optical aberrations of optical systems without rotational symmetry: spherical aberration," J. Opt. Soc. Am. A **26**, 1090–1100 (2009).
14. K. P. Thompson, "Multinodal fifth-order optical aberrations of optical systems without rotational symmetry: the comatic aberrations," J. Opt. Soc. Am. A **27**, 1490–1504 (2010).
15. K. P. Thompson, "Multinodal fifth-order optical aberrations of optical systems without rotational symmetry: the astigmatic aberrations," J. Opt. Soc. Am. A **28**, 821–836 (2011).
16. K. Fuerschbach, "Freeform, ϕ-polynomial optical surfaces: optical design, fabrication and assembly," Ph.D. thesis (University of Rochester, 2014).
17. A. Bauer and J. P. Rolland, "Design of a freeform electronic viewfinder coupled to aberration fields of freeform optics," Opt. Express **23**, 28141–28153 (2015).
18. A. Bauer and J. P. Rolland, "Visual space assessment of two all-reflective, freeform, optical see-through head-worn displays," Opt. Express **22**, 13155–13163 (2014).
19. A. Bauer, E. M. Schiesser, and J. P. Rolland, "Concurrent engineering of a next-generation freeform telescope: optical design," Proc. SPIE **10998**, 109980W (2019).
20. J. Reimers, A. Bauer, K. P. Thompson, and J. P. Rolland, "Freeform spectrometer enabling increased compactness," Light Sci. Appl. **6**, e17026 (2017).
21. R. W. Gray, C. Dunn, K. P. Thompson, and J. P. Rolland, "An analytic expression for the field dependence of Zernike polynomials in rotationally symmetric optical systems," Opt. Express **20**, 16436–16449 (2012).
22. Synopsys Inc., *CODE V Lens System Setup Reference Manual* (Synopsys Inc., 2017).
23. N. Takaki, A. Bauer, and J. P. Rolland, "On-the-fly surface manufacturability constraints for freeform optical design enabled by orthogonal polynomials," Opt. Express **27**, 6129–6146 (2019).
24. "Appendix A Zernike Polynomials," in *CODE V Lens System Setup Reference Manual* (Synopsys Inc., 2018), p. 573.
25. J. Sasian, "Interpretation of pupil aberrations in imaging systems," Proc. SPIE **6342**, 634208 (2006).
26. J. M. Hoffman, "Induced aberrations in optical systems," Ph.D. dissertation (University of Arizona, 1993).